Generating mouse models of degenerative diseases using Cre/lox-mediated in vivo mosaic cell ablation

Masato Fujioka,[1,2,3,4] Hisashi Tokano,[1,2] Keiko Shiina Fujioka,[1,2] Hideyuki Okano,[3] and Albert S.B. Edge[1,2,5]

[1]Department of Otology and Laryngology, Harvard Medical School, Boston, Massachusetts, USA. [2]Eaton-Peabody Laboratory, Massachusetts Eye and Ear Infirmary, Boston, Massachusetts, USA. [3]Department of Physiology and [4]Department of Otolarnygology, Head and Neck Surgery, Keio University School of Medicine, Tokyo, Japan. [5]Program in Speech and Hearing Bioscience and Technology, Division of Health Science and Technology, Harvard and Massachusetts Institute of Technology, Cambridge, Massachusetts, USA.

Most degenerative diseases begin with a gradual loss of specific cell types before reaching a threshold for symptomatic onset. However, the endogenous regenerative capacities of different tissues are difficult to study, because of the limitations of models for early stages of cell loss. Therefore, we generated a transgenic mouse line (*Mos-iCsp3*) in which a lox-mismatched Cre/lox cassette can be activated to produce a drug-regulated dimerizable caspase-3. Tissue-restricted Cre expression yielded stochastic *Casp3* expression, randomly ablating a subset of specific cell types in a defined domain. The limited and mosaic cell loss led to distinct responses in 3 different tissues targeted using respective Cre mice: reversible, impaired glucose tolerance with normoglycemia in pancreatic β cells; wound healing and irreversible hair loss in the skin; and permanent moderate deafness due to the loss of auditory hair cells in the inner ear. These mice will be important for assessing the repair capacities of tissues and the potential effectiveness of new regenerative therapies.

Introduction

Most degenerative diseases are initiated by gradual losses of particular cell types. In contrast to acute diseases, degenerative disorders usually proceed through a presymptomatic stage before reaching a threshold for the onset of disease: in type 1 diabetes, hyperglycemia commonly develops when approximately 80% of the β cells are lost (1); in Parkinson disease, motor dysfunction commences when tyrosine hydroxylase-positive neurons in the substantia nigra are decreased by 70%–80% (2). The threshold differs among organs depending on their reserve capacity and on the extent of endogenous cell replacement normally occurring in that tissue.

To investigate the loss of specific cell types in vivo, techniques for genetic ablation within particular cells or lineages have been developed using specific gene control elements (3–8). Conditional ablation is an indispensable tool in biology for examining the function of individual cell types. However, none of these models recreate the gradual progress of degeneration from the earliest time of symptomatic onset that can reproducibly lead to limited, partial cell ablation that would help to understand early stages of disease.

Here, we have created a transgenic mouse, *Mos-iCsp3*, to ablate subsets of specific cell types in a mosaic pattern. An inducible suicide gene was expressed within a domain defined by Cre expression, but, by using a previously reported lox-mismatched Cre/lox expression cassette (9), a mosaic pattern of cell death was achieved. In many degenerative diseases, cell death occurs through apoptosis. To investigate the process of degenerative disease after cell loss, we decided to use an engineered, dimerizable human caspase-3 to recapitulate physiological apoptotic cell death. The caspase gene was fused to 2 tandem FK506-binding sites (Fvs) and served as the conditional suicide gene, such that activation via dimerization was induced by an FK506 analogue (AP20187) that brings the 2 monomers together through an Fv-dimerizer-Fv complex (10). This process was quick and could be tightly controlled, because the protein remains in the cytoplasm but does not dimerize until the signal is provided.

By crossing this transgenic mouse with 3 different Cre mice, *Ins2-Cre*, *Krt14-CreER*, and *Pou4f3-Cre*, we successfully obtained reproducible impaired glucose tolerance, with normal glycemia that is relevant to a prediabetic stage; mild skin damage, followed by healing but permanent loss of hairs; and irreversible moderate deafness due to the loss of auditory hair cells, respectively. All 3 double-transgenic mice suffered partial but specific depletion of target cell types with moderate symptoms, demonstrating the applicability of this model for recapitulating early stages of disease. In contrast, individual tissue responses differed: while death of islets of *Ins2-Cre;Mos-iCsp3* mice and death of epidermis in *Krt14-CreER;Mos-iCsp3* mice were accompanied by cell replacement, regrowth of hair in the latter was limited. In *Pou4f3-Cre;Mos-iCsp3* mice, auditory hair cells did not recover and mild deafness was permanent.

Reproducible models of cell death are useful for understanding disease and will help understanding of tissue repair or regeneration. Testing regenerative protocols requires that the models be reproducible so that the treatment can be compared with controls with little variation. Our results clearly demonstrated disparate responses that corresponded to the capacity for spontaneous restoration or regeneration in 3 different targeted tissues. Collectively, the data indicate that the method could be applicable to the testing of approaches for repair of tissues that lack spontaneous regenerative capacity.

Results

Double-inducible cell ablation was tightly controlled by Cre-mediated recombination and caspase dimerization. To obtain a mouse that could generate multiple models of tissue-specific and mosaic cell death, we placed a previously reported flox-stop expression plasmid (9)

Conflict of interest: The authors have declared that no conflict of interest exists.
Citation for this article: *J Clin Invest.* 2011;121(6):2462–2469. doi:10.1172/JCI45081.

that gives rise to mosaic expression due to the lox-mismatch and CMV promoter after recombination in vivo in combination with an expression cassette (Figure 1A). We constructed the transgene, *Mos-iCsp3*, by inserting an inducible, dimerizable caspase-3 gene (*pSH-MFv2Csp3E*) downstream of the flox-stop expression cassette.

The capacity for cell ablation was tested by LIVE/DEAD analyses (Invitrogen). Transfection of the parental vector followed by treatment with AP20187 induced death in 696.5×10^6 cells/μm^2 as compared with 161.3×10^6 cells/μm^2 in control cultures (Supplemental Figure 1, A and B; supplemental material available online with this article; doi:10.1172/JCI45081DS1). When cotransfected with *Mos-iCsp3* and Cre, the number of ethidium-D1–positive dying cells was increased from 146.7×10^6 cells/μm^2 to 601.2×10^6 cells/μm^2 after addition of AP20187, approximately 80% of the value for cells transfected with the parental vector (Supplemental Figure 1C). Inducibility of the system was measured by MTT assay, as described in Supplemental Methods. A significant decrease in cell number was observed in cells treated with AP20187 ($P < 0.01$) but not in cells cotransfected with Cre and *Mos-iCsp3* without AP20187 (Supplemental Figure 1D). These data showed that cell ablation by *Mos-iCsp3* was controlled by Cre-recombinase expression plus AP20187 administration.

Mosaic-patterned expression of iCsp3 in the Mos-iCsp3 transgenic mouse. After confirmation of transgene function in vitro, we generated a transgenic mouse, *Mos-iCsp3*, and selected founder lines (Supplemental Figure 2). Transgene expression in various organs of individual lines was examined by β-galactosidase assay and immunostaining for V5-tag (Supplemental Figure 3 and Supplemental Table 1). Recombination induced by Cre recombinase could be observed and was not complete, as expected (Supplemental Figure 4).

Dimerizer induced impaired glucose intolerance but not diabetes in Ins2-Cre; Mos-iCsp3 double transgenics. Pancreatic β cells produce insulin to control the level of blood sugar. We first used our transgenic mouse to recapitulate the prediabetic state by direct but limited ablation of β cells. We analyzed the functional depletion by measuring blood sugar. The *Mos-iCsp3* mouse was crossed with an *Ins2-Cre* mouse, which expresses Cre in β cells, and resulted in mosaic-patterned expression of the *Mos-iCsp3* transgene specifically in target cells. The percentage of insulin-positive cells that expressed iCsp3, as revealed by anti-HA tag immunostaining, was 72.3% ± 1.5% (Supplemental Figure 5 and Supplemental Table 2).

Time-dependent changes in blood sugar in the double-transgenic (*Ins2-Cre;Mos-iCsp3*) mice and littermates were examined at 18 hours and at 1, 2, 3, 5, and 40 days after AP20187 administration (Figure 1B). No difference was observed between groups at any time point, indicating that the double transgenic was normoglycemic even after dimerizer treatment (Figure 1C). In contrast, the glucose tolerance test showed striking changes: the blood glucose level of double transgenics or littermate controls was examined before and 5, 15, 30, 60, and 120 minutes after intraperitoneal injection of glucose and before and 5 and 40 days after AP20187 injection. Blood sugar levels were significantly higher in double-transgenic mice compared with those in controls, while no differences were observed before the injection (Figure 1, D–F). Islet size was evaluated by immunostaining for insulin (Figure 1, G and H). As early as 12 hours after the injection of AP20187, islet size began to decrease, which was consistent with a previous report showing that in vivo activation of caspase-3 fusion protein was observed from 3 hours until 24 hours after injection of AP20187 (6). Ten days after injection of AP20187, the size of the islets was significantly decreased from 193.75 ± 41.6 pixels/field to 82.5 ± 19.5 pixels/field, a decrease of 57.4%. Note that the islets in double transgenics were larger at day 40 of AP20187, which is consistent with previous reports demonstrating proliferation in response to damage to β cells (11). A return of the glucose tolerance test to near normal in parallel with the increase in the number of insulin-positive cells indicated that hyperplasia led to a partial restoration of normoglycemia.

Dimerizer-induced punctate lesions in the skin of Krt14-CreER;Mos-iCsp3 mice were reversible and partial hair loss was not reversed. The skin, including epidermis and hair, provides a barrier that must be renewed to be effective. Cells in the epidermis are replaced throughout life, especially after injury or loss of cells, by stem cells called basal cells, which are at the bottom of the epidermis, and hair is replaced by stem cells residing in "bulges" in the hair follicle. The bulge stem cells have the ability to reconstitute all of the hair structures (12, 13) and divide only at the onset of periods of hair growth. We chose to evaluate the phenotype in the skin after mating *Mos-iCsp3* mice with *Krt14-CreERT2*, in which tamoxifen-inducible Cre-recombinase is expressed both in the epidermis and in the hair follicles, including outer root sheath and bulges.

Double transgenics were clipped in their mid-dorsal area at P49, when the hair cycle was in the second telogen stage, and we administered 4-OH tamoxifen to half of the dorsal skin topically for 14 days (14). This timing of this procedure covers the telogen to anagen transition (13), as confirmed by the pale pink color of the skin in pigmented littermates after clipping. The treatment led to spatially restricted expression of inducible caspase, as confirmed by staining for the HA tag. HA expression could be seen in 62.9% ± 8.4% of the epidermal cells, including hair follicles (Supplemental Figure 5 and Supplemental Table 2). After the 4-OH tamoxifen treatment, AP20187 was injected intraperitoneally daily for 2 sequential days. Before and 0, 1, 2, 7, 14, 35, and 49 days after the administration of dimerizer, the gross appearance of the skin was examined (Figure 2, B and C), followed by histopathological evaluation at each time point (n = 4, 2, 3, 2, 2, 3, 3, and 3 mice, respectively). At day 1, most of the mice (12 out of 13 mice) suffered apparent changes in gross skin appearance, including the emergence of eruptions and redness (Figure 2B and Supplemental Figure 6). Histological evaluation revealed that lesions included scattered pyknotic cells in the epidermis, both within the stratum granulosum and, notably, in the polygonal cells of the stratum spinosum (Figure 2F). Fifty percent of the cells in the stratum spinosum and basal epidermis in the 4-OH tamoxifen–treated area were positive for apoptosis, as determined by single-stranded DNA (ssDNA) immunostaining to visualize fragmented DNA (Figure 2E). In addition to the epidermis, the lower portion of the hair follicles in the bulge region, where follicle stem cells reside, also expressed the transgene after recombination. Focal alopecia was seen in the area treated with 4-OH tamoxifen at later time points, when hair growth or regrowth was obtained in the rest of the area in the same mice (Figure 2C and Supplemental Figure 6). Histopathology of the skin at day 1 showed that 46.1% of the bulge cells were positive for staining with the antibody to ssDNA (Figure 2E). Ablation of stem cells in the bulge region has been shown previously to block the regrowth of hair (15). It thus appeared that in vivo depletion of stem cell pools in the hair follicle bulge area in the transgenic mice led to focal alopecia, providing a model of a "shortage of supply" of stem cells.

Dimerizer-induced inner ear hair cell–specific mosaic ablation led to reproducible, permanent hearing loss in Pou4f3-Cre;Mos-iCsp3 double-transgenic mice. The hair cells in the cochlea are the primary cells

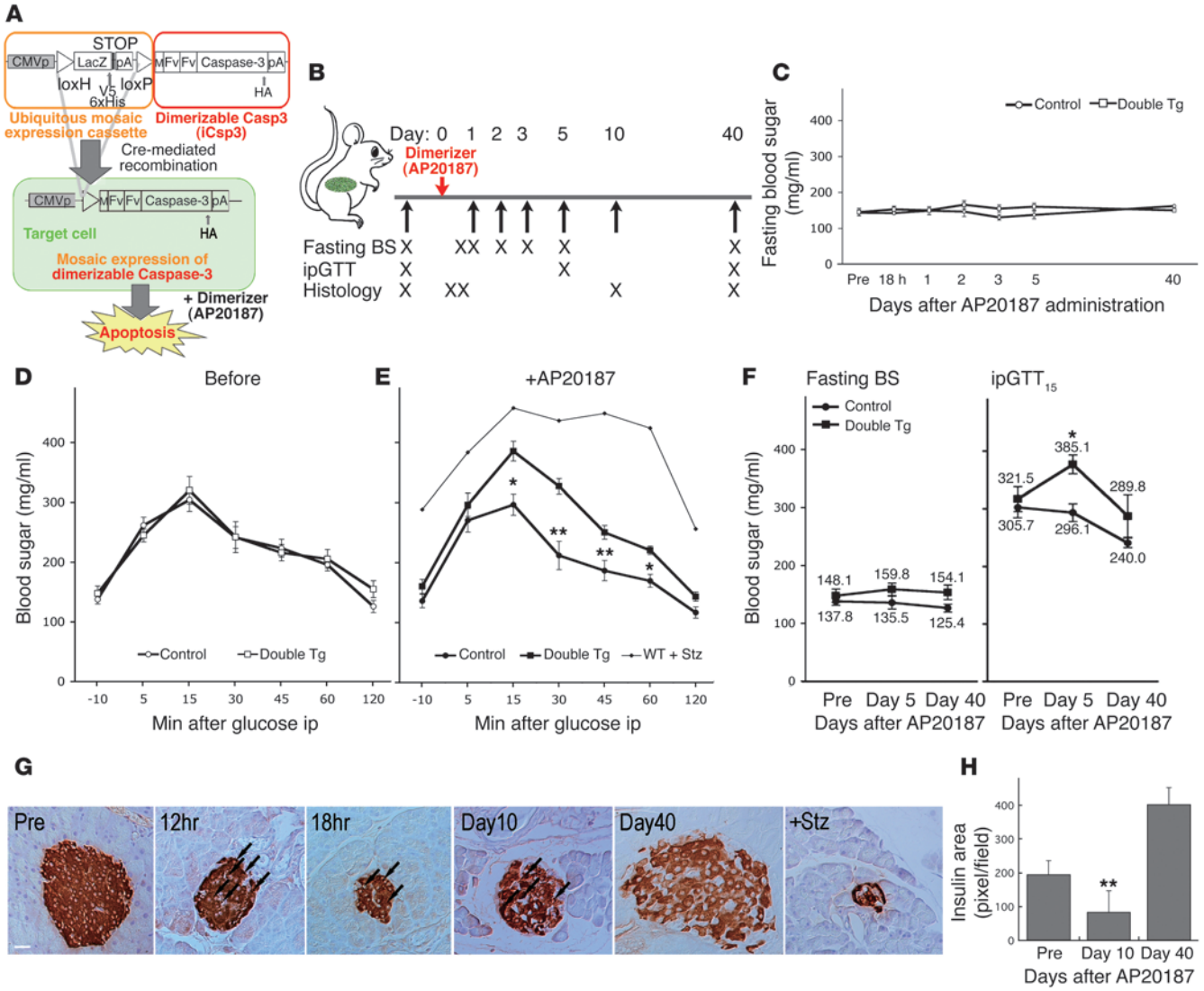

Figure 1

Mosaic ablation of pancreatic β cells led to impaired glucose tolerance. (**A**) Plan for the cell ablation experiments. (**B**) Experimental design for mosaic ablation of pancreatic β cells using a double-transgenic *Ins2-Cre;Mos-iCsp3* mouse. BS, blood sugar; ipGTT, i.p. glucose tolerance test. (**C**) Time course of fasting blood sugar in double transgenics (Cre/Csp) and littermate controls. There were no significant differences in the fasting blood sugar in 2 groups at any time point. (**D** and **E**) Glucose tolerance test of (**E**) double-transgenic mice and (**D**) littermate controls. Blood sugar was elevated in double transgenics only after intraperitoneal glucose injection (1 mg/g body weight) compared with that in littermates after AP20187 treatment, while there were no differences before dimerizer treatment. Note that the glucose level was highly elevated in wild-type mice treated with streptozotocin (Stz), both fasting and after glucose loading. (**F**) Fasting blood sugar level and glucose tolerance test 15 minutes after loading. (**G**) Gross histology of pancreatic β cells in double transgenics. Many islet cells had pyknotic nuclei in a mosaic distribution at day 10 (black arrows), suggesting that dimerizer had induced stochastic apoptosis of β cells. Note that no apoptotic cells were found, but the size of the islet was larger at day 40 than that in pretreatment, which is consistent with other reported models for specific β cell ablation. Scale bar: 20 μm. (**H**) Quantification of the insulin immunopositive area at different time points. A significant decrease in the insulin-positive area was observed at day 10 compared with that in pre-AP20187–treated control double transgenics. $^{*}P < 0.05$, $^{**}P < 0.01$.

for mechanosensory transduction and generate action potentials in response to vibration from sound. The hair cells are arranged in an unusual pattern in the organ of Corti to form a single plane in 1 and 3 rows of inner and outer hair cells, respectively. Hair cells are surrounded by another cell type, the supporting cells. The regular alternating pattern is particularly suitable for understanding the distribution of the recombined cells. We obtained a hair cell–specific mosaic expression of inducible caspase by mating a *Mos-iCsp3* mouse with a *Pou4f3-Cre* mouse, which was confirmed by immunostaining for the HA-tag: 63.5% ± 6.6% of myosin VIIa-positive hair cells expressed iCsp3 in the perinatal organ of Corti (Supplemental Figure 5).

We assessed cell ablation by analyzing this natural geometric pattern in *Pou4f3-Cre* mice crossed with *Math1-nGFP* hair cell reporter mice that were maintained as double homozygotes so that hair cells expressed both Cre-recombinase and nuclear-local-

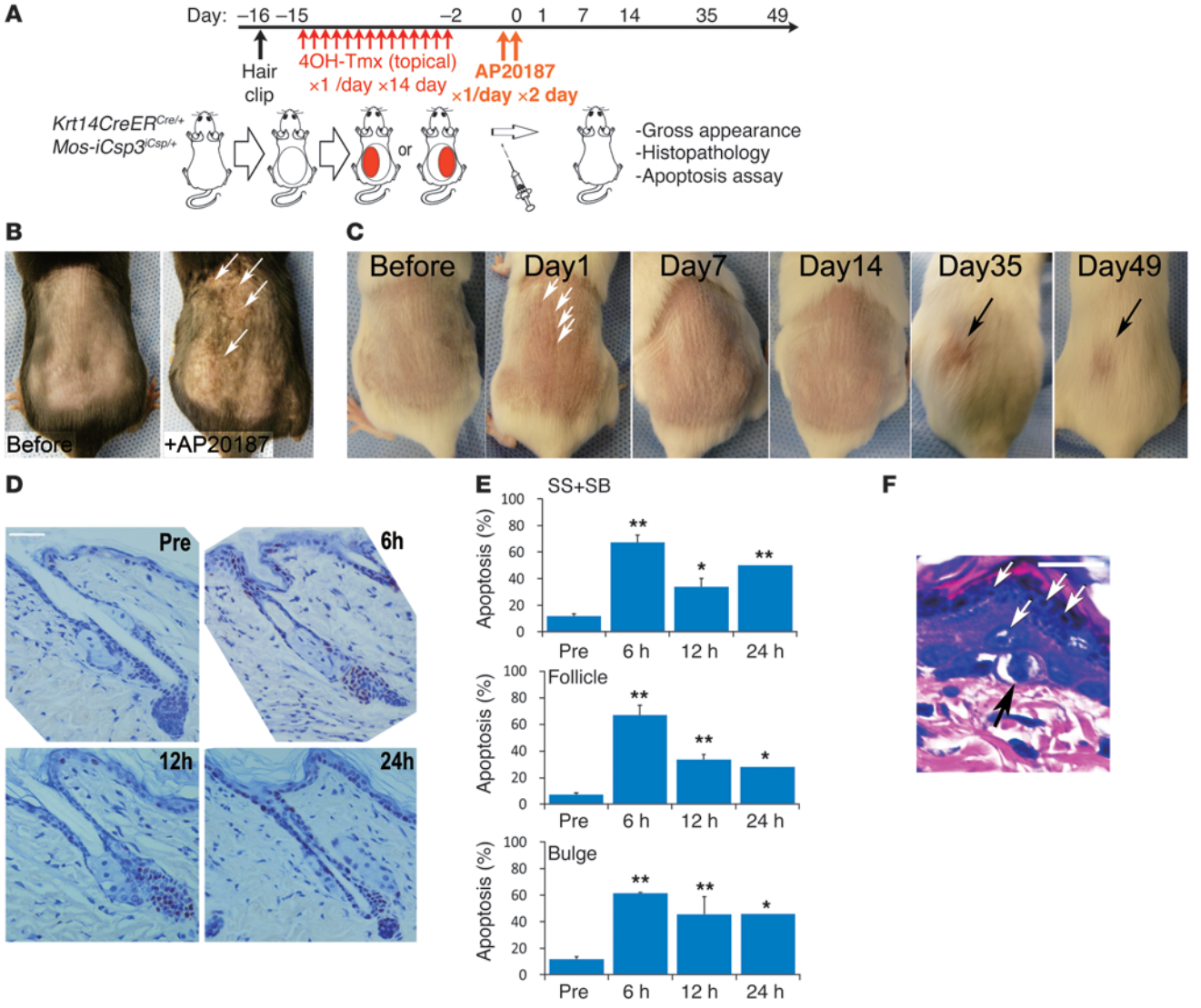

Figure 2

In vivo ablation of skin cells in *Krt14-CreER;Mos-iCsp3* double transgenics. (**A**) Experimental design (n = 13). 4OH-Tmx, 4-OH tamoxifen. (**B**–**F**) In vivo ablation of skin cells. After AP20187 injection, a mild wound was observed in the area where 4-OH tamoxifen had been topically applied, including eruption and a punctate red lesion (white arrows in **B** and **C**). Five to six weeks after AP20187, most of the hair in the clipped lesion had been replaced, while the 4-OH tamoxifen–treated area had lost hair (black arrows in **C**). (**D**) Apoptotic cells visualized by immunostaining for ssDNA were found in the area of 4-OH tamoxifen treatment. Apoptosis was evident 6 hours after the last injection of AP20187. (**E**) At day 1, 50.1% of epidermis and 46.1% of bulge cells had undergone apoptosis. (**F**) In epidermis, dividing basal cells were frequently observed at the bottom of the 4-OH tamoxifen–treated area (black arrow). White arrows indicate dying cells induced by AP20187 treatment. Scale bar: 50 μm (**D**); 20 μm (**F**). *P < 0.05, **P < 0.01.

ized GFP (16). The organs of Corti of triple-transgenic mice or littermates were harvested at P3, plated flat on a poly-L-lysine–coated dish, and incubated with 10 nM AP20187 or DMSO (Figure 3A). Time-dependent changes in hair cell distribution were examined before and 12, 24, 48, and 72 hours after the addition of AP20187 by observing GFP fluorescence (Figure 3, C and D). The number of hair cells was decreased only in triple transgenics treated with AP20187; no significant difference was observed in littermates lacking the *Mos-iCsp3* allele treated with AP20187 compared with *Math1-nGFP* control cultures (Figure 3D). The ablation was reproducibly completed within 48 hours and remained unchanged for the next 24 hours (Figure 3E). Loss of hair cells was observed in a mosaic pattern (Figure 3, C and D). At 72 hours, the number of nuclear GFP–positive (nGFP-positive) cells was decreased to 49.5% ± 1.6% and 94.6% ± 2.5% in double transgenics with nGFP reporter and controls lacking *Mos-iCsp3*, respectively (Figure 3F), and was statistically significant (P < 0.05). Further counting in fixed tissue showed that the number of surviving hair cells in the triple transgenics was significantly lower than that in the controls (32.0 ± 2.3 cells/100 μm vs. 54.7 ± 2.7 cells/100 μm in the 16-kHz region; P < 0.05), while supporting cell numbers were not altered (66.7 ± 1.3 cells/100 μm vs. 69.0 ± 3.0 cells/100 μm; Figure 3G). Morphological observation with staining showed that cell ablation was accompanied by decay of structural pro-

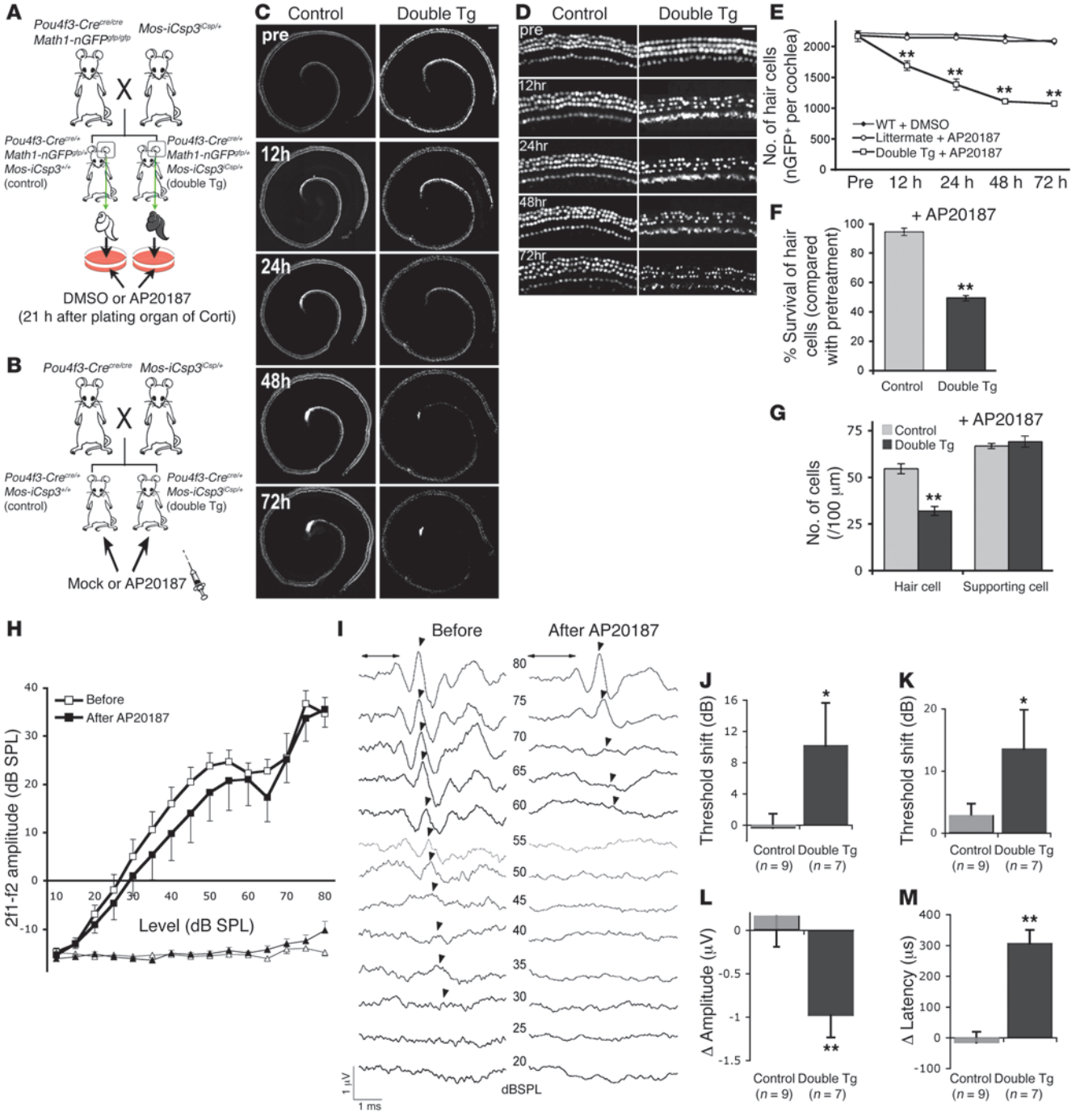
A
Pou4f3-Cre cre/cre Math1-nGFP gfp/gfp
Mos-iCsp3 iCsp/+
Pou4f3-Cre cre/+ Math1-nGFP gfp/+ Mos-iCsp3 +/+ (control)
Pou4f3-Cre cre/+ Math1-nGFP gfp/+ Mos-iCsp3 iCsp/+ (double Tg)
DMSO or AP20187
(21 h after plating organ of Corti)
B
Pou4f3-Cre cre/cre Mos-iCsp3 iCsp/+
Pou4f3-Cre cre/+ Mos-iCsp3 +/+ (control)
Pou4f3-Cre cre/+ Mos-iCsp3 iCsp/+ (double Tg)
Mock or AP20187
C
Control
Double Tg
pre
12h
24h
48h
72h
D
Control
Double Tg
pre
12hr
24hr
48hr
72hr
E
No. of hair cells (nGFP+ per cochlea)
WT + DMSO
Littermate + AP20187
Double Tg + AP20187
Pre 12 h 24 h 48 h 72 h
F
+ AP20187
% Survival of hair cells (compared with pretreatment)
Control
Double Tg
G
+ AP20187
Control
Double Tg
No. of cells (/100 μm)
Hair cell
Supporting cell
H
Before
After AP20187
2f1-f2 amplitude (dB SPL)
Level (dB SPL)
I
Before
After AP20187
dBSPL
1 μV
1 ms
J
Threshold shift (dB)
Control Double Tg
(n = 9) (n = 7)
K
Threshold shift (dB)
Control Double Tg
(n = 9) (n = 7)
L
Δ Amplitude (μV)
Control Double Tg
(n = 9) (n = 7)
M
Δ Latency (μs)
Control Double Tg
(n = 9) (n = 7)
N
+ Mock
+ AP20187
Pv3 (Hair cells)
ToPro-3(nuclei)
double Tg
double Tg
O
Double Tg
% Hair cell loss
IHC
OC1
OC2
OC3
P
+ AP20187
Spiral ganglion density (×10³/μm²)
Control
Double Tg

Figure 3
In vitro and in vivo ablation of auditory hair cells in *Pouf4f3-Cre;Mos-iCsp3* double transgenics. (**A** and **B**) Experimental design. (**C**–**G**) In vitro ablation of hair cells in organ of Corti explant culture ($n = 4$ in each group). (**C** and **D**) Nuclei of hair cells were visualized by EGFP. (**D** and **E**) A significant decrease in hair cells was observed only in double transgenics treated with AP20187 and was apparent at 12 hours. (**F**) At 72 hours, GFP-positive hair cells were decreased to 49.5% ± 1.6% in double transgenics. (**G**) The number of supporting cells was unaffected. (**H**–**M**) Functional changes in the auditory system were measured (25) by (**H** and **J**) DPOAE and (**I** and **K**–**M**) ABR. Amplitude, peak I latency (**I**, horizontal line), and threshold (**I**, arrowheads) of the ABR are shown at 16 kHz: significant but moderate deafness was induced only in double transgenics after AP20187 administration ($n = 9$ and 7 in control and double-transgenic groups, respectively). (**N**–**P**) Histological changes in the cochlea ($n = 3$ and 6 in control and double-transgenic groups, respectively). (**N**) Mosaic-patterned partial hair cell loss (white arrows) was observed in double transgenics treated with AP20187, confirmed by Pv3 immunostaining and loss of nuclei. The bottom right panel in **N** was composed from 2 images. (**O**) Quantification showed 29.3% ± 3.2% of inner hair cells (IHCs) and 23.2% ± 2.6% of outer hair cells (OC1–OC3) were lost, (**P**) while the density of spiral ganglion neurons was not changed. All data were collected in the 16-kHz area before or 7 days after AP20187 administration. $^*P < 0.05$, $^{**}P < 0.01$. Scale bar: 50 μm (**C**); 20 μm (**D** and **N**).

teins, including myosin VIIa (Supplemental Figure 7, A and B), followed by the ejection of shrinking hair cells to the luminal surface and ingrowth of surrounding supporting cells (Supplemental Figure 7, A, E, F, and G). These data clearly demonstrated the specificity of cell ablation in hair cells of *Pou4f3-Cre;Mos-iCsp3* mice and showed that the ablation was tightly defined by exposure to dimerizer and occurred in a mosaic pattern, followed by a wound-healing response by surrounding supporting cells but not by hair cell replacement (Supplemental Figure 7H).

Primary loss of hair cells is a major cause of deafness (17, 18), but strict hair cell–specific ablation using genetic modification has not been reported. We determined whether the transgenic mouse could serve as a model for early stages of deafness due to hair cell loss in vivo by examining auditory function and the number of hair cells in *Pou4f3-Cre;Mos-iCsp3* double transgenics (Figure 3B). At 6 weeks of age, double transgenics exhibited a slight decrement (Figure 3H) in distortion product otoacoustic emission (DPOAE), a measure of outer hair cell function, with a small but significant elevation of threshold (27.5 ± 3.5 dB before AP20187 and 36.0 ± 9.2 dB after AP20187, measured at 7 days, a shift of 8.5 dB; $P < 0.01$), while no significant changes (–0.33 dB shift) were observed in controls (Figure 3J). The auditory brainstem response (ABR) also indicated moderate impairment of hearing in double-transgenic mice after AP20187 treatment (Figure 3I). In contrast with the control animals, wave I latency (1.35 ± 0.08 ms before AP20187 and 1.68 ± 0.14 ms after AP20187), peak-to-peak amplitude (2.48 ± 0.65 μV before AP20187 and 1.64 ± 0.51 μV after AP20187), and hearing thresholds (29.2 ± 2.2 dB before AP20187 and 44.2 ± 9.3 dB after AP20187) ($P < 0.01$) were significantly deteriorated in response to AP20187 (Figure 3, K–M). Histological examination showed a mosaic-patterned hair cell loss (Figure 3N). Loss of hair cells in vivo was 24.6% ± 1.8% (Figure 3, N and O, and Supplemental Figure 8), and no significant change was observed in spiral ganglion neurons (Figure 3P). These data clearly demonstrated that a stochastic partial ablation that was specific to hair cells was induced by AP20187 administration in *Pou4f3-Cre;Mos-iCsp3* double-transgenic mice and led to moderate but reproducible deafness. Note that the ablation was permanent, presumably due to the lack of spontaneous regeneration of mammalian auditory hair cells.

Discussion

In this paper, we describe a transgenic mouse that can be used for cell ablation in cells that have been engineered to express a caspase gene controlled by addition of a chemical dimerizer to generate models of degenerative disease by mosaic-patterned stochastic cell death.

Target cells are defined by 3 factors: the expression pattern of the transgene, the choice of Cre mouse, and the site of delivery of chemical dimerizer. Although the *Mos-iCsp3* transgene is driven by a ubiquitous promoter, expression varies among lines. This feature has been used to fine-tune transgene expression to more specifically target tissues in which expression of the caspase construct and Cre intersect: for example, to restrict cell death to areas of the central nervous system outside the cerebellum when using a Cre that was widely expressed in the brain, use of line 11, which had no expression in cerebellum, would be helpful. Dimerizer may also be restricted to a cell type of choice: targets inside the blood-brain barrier can be selected by dimerizer administration into the intracerebral space.

This transgenic allows us to create ablation models for numerous specific tissues by crossing with the appropriate Cre-expressing mice. The approach has several advantages over previous methods, because the caspase gene is expressed in any tissue that can be targeted by a Cre mouse and is inducible, with activation controlled by administration of dimerizer. It is also notable that the amount of transgene expression in target cells is not defined by a tissue-specific promoter. A strong promoter to drive expression has an advantage over tissue-specific promoters or loci that can be weak in transgenic or knock-in Cre mice, respectively, and strong and accurate gene regulatory elements are not available for many tissues. Moreover, in this system, the Cre recombinase only "turns the switch" by excising a stop sequence but does not cause cell death until dimerizer is administered. This feature allowed use of *Pou4f3-Cre*, which is expressed transiently in embryonic stages, to prepare for the iCsp3 expression prior to the actual experiment in the adult, giving access to a broader selection of tissues for specific ablation, including those marked by genes expressed in specific tissues during development.

Most degenerative diseases begin with partial loss of specific cells. Our transgenic model facilitates investigation of the "onset" of degenerative disease, providing a picture of the extent of cell loss when a symptom first becomes apparent and the disease is in its early stages. Use of caspase and dimerization, the normal mechanism for activation, provided a model of physiological cell death and was similar to actual degeneration, since there was no inflammation and cells adjacent to the targeted cells were unaffected. The approach has an advantage over methods using toxins, in which cell damage precedes cell death and a cell might be damaged but not undergo cell death if the level of toxin was insufficient. Cell death in cells that expressed the recombined caspase transgene was rapid and complete, and the ablation pattern was stochastic; the number of cells lost within a cell type defined by Cre was reproducible. This point is important for a degenerative model that is to be used for testing approaches to regeneration. This has been difficult to study in the available

models that cause extensive damage that is variable and difficult to control (12, 13, 19). We used AP20187 at 0.5 mg/kg, because Mallet et al. showed that damage reached a plateau above this dose (6): lower doses of AP20187 may also be useful to induce different levels of cell death, recapitulating earlier time points of disease. Interestingly, cell ablation had proceeded to a similar degree in the 3 double-transgenic models tested (Supplemental Tables 2 and 3) but resulted in strikingly different functional outcomes. This difference reflects the individual tissues' ability to regenerate spontaneously following injury, which has been difficult to trace in many tissues, particularly if a stem cell compartment has not been observed. In *Ins2-Cre;Mos-iCsp* double transgenics, glucose tolerance was markedly reduced and sustained. Hyperplasia of islets that were partially destroyed by the loss of β cells was caused by proliferation of the remaining islets (11, 20, 21) and led to a slow return of euglycemia in these animals. Regeneration in response to cell death in the islets was consistent with replacement either from progenitor cells in the ducts (20) or from division of existing β cells (5, 8, 11). In the inner ear, we saw no cell recovery and no new differentiation of hair cells after ablation of approximately 30% of the cells. This was consistent with the finding that there is no renewal mechanism for cells in the sensory organ for hearing and agrees with previously observed lack of regeneration of mammalian hair cells (17). In the skin, we destroyed cells that form a part of the stem cell compartment for hair production. The loss of bulge cells in a mosaic pattern resulted in alopecia where the damage was above a threshold level. This agrees with the finding that hair does not regrow after ablation of bulge stem cells in the hair follicle (15), although new hair follicle stem cells that can replace the follicle are produced after physical disruption of skin (13).

In summary, we have created a transgenic mouse model, which we believe to be novel, for mosaic but reproducible ablation of specific cell types. The model has several advantages: a mosaic pattern of cell loss recapitulates onset of degenerative disease; a wide variety of tissue ablation can be achieved with the broad range of Cre lines available; and, since cell death occurs only after administration of a drug, disease models can be obtained by crossing the caspase-3 mouse to Cre lines in which tissue-specific expression is found in the adult or the embryo. The different levels of functional amelioration in 3 different double-transgenic mice showed that elicitation of symptoms was dependent on the reserve cell number needed in a particular tissue and that the extent of cell replacement varied with tissue type. These noteworthy features will facilitate detailed investigation of degenerative disease and would be particularly useful in the exploration of new interventions that stimulate cell replacement.

Methods

Transgene construction. Inducible caspase-3 (iCsp3) gene was cloned by PCR from the previously reported plasmid (6) (*pSH-MFv2Caspase3E*; a gift from David Spencer, Baylor College of Medicine, Houston, Texas, USA), with the forward and reverse primers tagged with *Nhe I* and *Xba I*, respectively, and was subcloned into the respective sites of an inducible expression vector (9), carrying an expression cassette leading to the spatially mosaic distribution of the end product after the Cre-recombinase mediated removal of LacZ gene plus STOP sequence. The following oligonucleotides were used for the PCR: MFv2Casp3E forward, 5′-CCACCATGGGGAGTAGCAAGAG-3′ and, MFv2Casp3E reverse, 5′-GGAATTCTTAGTCGAGTGCGTAGT-3′.

In vitro inducible recombination and cell ablation assay. Cre-mediated in vitro recombination and AP20187-induced cell ablation was confirmed in vitro using HEK293 cells. See the Supplemental Methods for details.

Mice. The *Mos-iCsp3* transgene was separated by Pac I digestion, isolated with Qiaquick Gel Extraction Kits (Qiagen), and injected into fertilized oocytes of *C57BL/6;C3H/HeN* F1 hybrid mice at the Massachusetts General Hospital Transgenic Mouse Core Facility. Founder transgenic mice were identified by the analysis of tail genomic DNA and transgene expression of individual lines was assessed by both LacZ staining and β-galactosidase assay (Supplemental Figure 3 and Supplemental Table 1). Subsequently, 3 lines that consistently expressed LacZ throughout the body were established. Genotyping was performed following a previously reported protocol for the mosaic expression cassette used (9).

F1 to F3 *Mos-iCsp3* mice were mated with tissue-specific Cre mice. Based on the expression profiles in the Supplemental Methods, 2 lines were chosen and mated with respective tissue-specific Cre mice: for the ablation of pancreatic β cells in islets and epidermal cells of skin, line 14 was mated with an *Ins2-Cre* mouse (22) and a *Krt14-CreER* (14) mouse (The Jackson Laboratory), respectively. For the ablation of inner ear hair cells to create a deafness model, line 17 was mated with a *Pou4f3-Cre* mouse (23) (gift from Douglas Vetter, Tufts University, Boston, Massachusetts, USA). In each experiment, 6- to 8-week-old healthy double-transgenic mice were used. For in vitro organ culture experiments, the *Pou4f3-Cre* mouse was crossed with a *Math1-nGFP* reporter mouse (a gift from Jane Johnson, University of Texas, Dallas, Texas, USA) and maintained as a double homozygote. Expression of inducible caspase in each double transgenic was examined by immunostaining for the HA-tag. Apoptotic cells were visualized by ssDNA immunostaining (24). See the Supplemental Methods for details. All protocols were approved by the Institutional Animal Care and Use Committee of Massachusetts Eye and Ear Infirmary, in compliance with the Public Health Service policy on humane care and use of laboratory animals.

Statistics. Two-tailed Mann-Whitney U test was used to compare differences among treatment groups. Changes before and after treatment of the same animal were analyzed by 2-tailed Wilcoxon *t* test. Repeated-measures ANOVA was used to compare time-dependent differences among groups. Data are presented in the text and in figures as mean ± SEM. *P* values of less than 0.05 were considered significant.

Acknowledgments

We are grateful to K. Darrow for instruction on surgical methods, to K. Takahashi for instruction on histopathology of the skin, to the Dana-Farber Rodent Histopathology Core for assistance with histopathology of skin and pancreas, and to J. Forrester, C. Miller, and L. Liberman for technical assistance. We thank M.C. Liberman and A. Brugeaud for critical discussions. This work was supported by grants RO1 DC007174, R21 DC010440-01, and P30 DC05209 from the National Institute on Deafness and Other Communicative Disorders; by Grant-in-Aid for Young Scientists (B) from the Japanese Ministry of Education, Culture, Sports, Science and Technology to M. Fujioka; by Keio Gijuku Fukuzawa Memorial Fund for the Advancement of Education and Research to M. Fujioka; and by the Hamilton H. Kellogg and Mildred H Kellogg Charitable Trust.

Received for publication September 11, 2010, and accepted in revised form March 2, 2011.

Address correspondence to: Albert Edge, Eaton-Peabody Laboratory, Massachusetts Eye and Ear Infirmary, 243 Charles Street, Boston, Massachusetts 02114, USA. Phone: 617.573.4452; Fax: 617.720.4408; E-mail: albert_edge@meei.harvard.edu.

1. Weir GC, Bonner-Weir S, Leahy JL. Islet mass and function in diabetes and transplantation. *Diabetes*. 1990;39(4):401–405.
2. Bernheimer H, Birkmayer W, Hornykiewicz O, Jellinger K, Seitelberger F. Brain dopamine and the syndromes of Parkinson and Huntington. Clinical, morphological and neurochemical correlations. *J Neurol Sci*. 1973;20(4):415–455.
3. Brockschnieder D, Pechmann Y, Sonnenberg-Riethmacher E, Riethmacher D. An improved mouse line for Cre-induced cell ablation due to diphtheria toxin A, expressed from the Rosa26 locus. *Genesis*. 2006;44(7):322–327.
4. Buch T, et al. A Cre-inducible diphtheria toxin receptor mediates cell lineage ablation after toxin administration. *Nat Methods*. 2005;2(6):419–426.
5. Cano DA, et al. Regulated beta-cell regeneration in the adult mouse pancreas. *Diabetes*. 2008; 57(4):958–966.
6. Mallet VO, et al. Conditional cell ablation by tight control of caspase-3 dimerization in transgenic mice. *Nat Biotechnol*. 2002;20(12):1234–1239.
7. Matsumura H, Hasuwa H, Inoue N, Ikawa M, Okabe M. Lineage-specific cell disruption in living mice by Cre-mediated expression of diphtheria toxin A chain. *Biochem Biophys Res Commun*. 2004;321(2):275–279.
8. Nir T, Melton DA, Dor Y. Recovery from diabetes in mice by beta cell regeneration. *J Clin Invest*. 2007;117(9):2553–2561.
9. Moeller MJ, Soofi A, Sanden S, Floege J, Kriz W, Holzman LB. An efficient system for tissue-specific overexpression of transgenes in podocytes in vivo. *Am J Physiol Renal Physiol*. 2005;289(2):F481–F488.
10. Chen M, Orozco A, Spencer DM, Wang J. Activation of initiator caspases through a stable dimeric intermediate. *J Biol Chem*. 2002;277(52):50761–50767.
11. Dor Y, Brown J, Martinez OI, Melton DA. Adult pancreatic beta-cells are formed by self-duplication rather than stem-cell differentiation. *Nature*. 2004;429(6987):41–46.
12. Fuchs E. The tortoise and the hair: slow-cycling cells in the stem cell race. *Cell*. 2009;137(5):811–819.
13. Ito M, et al. Wnt-dependent de novo hair follicle regeneration in adult mouse skin after wounding. *Nature*. 2007;447(7142):316–320.
14. Vasioukhin V, Degenstein L, Wise B, Fuchs E. The magical touch: genome targeting in epidermal stem cells induced by tamoxifen application to mouse skin. *Proc Natl Acad Sci U S A*. 1999;96(15):8551–8556.
15. Ito M, et al. Stem cells in the hair follicle bulge contribute to wound repair but not to homeostasis of the epidermis. *Nat Med*. 2005;11(12):1351–1354.
16. Lumpkin EA, et al. Math1-driven GFP expression in the developing nervous system of transgenic mice. *Gene Expr Patterns*. 2003;3(4):389–395.
17. Hildebrand MS, et al. Advances in molecular and cellular therapies for hearing loss. *Mol Ther*. 2008;16(2):224–236.
18. Ryals BM, Rubel EW. Hair cell regeneration after acoustic trauma in adult Coturnix quail. *Science*. 1988;240(4860):1774–1776.
19. Chien KR, Domian IJ, Parker KK. Cardiogenesis and the complex biology of regenerative cardiovascular medicine. *Science*. 2008;322(5907):1494–1497.
20. Inada A, et al. Carbonic anhydrase II-positive pancreatic cells are progenitors for both endocrine and exocrine pancreas after birth. *Proc Natl Acad Sci U S A*. 2008;105(50):19915–19919.
21. Nishio J, Gaglia JL, Turvey SE, Campbell C, Benoist C, Mathis D. Islet recovery and reversal of murine type 1 diabetes in the absence of any infused spleen cell contribution. *Science*. 2006;311(5768):1775–1778.
22. Postic C, et al. Dual roles for glucokinase in glucose homeostasis as determined by liver and pancreatic beta cell-specific gene knock-outs using Cre recombinase. *J Biol Chem*. 1999;274(1):305–315.
23. Sage C, et al. Essential role of retinoblastoma protein in mammalian hair cell development and hearing. *Proc Natl Acad Sci U S A*. 2006;103(19):7345–7350.
24. Korkolopoulou PA, Konstantinidou AE, Patsouris ES, Christodoulou PN, Thomas-Tsagli EA, Davaris PS. Detection of apoptotic cells in archival tissue from diffuse astrocytomas using a monoclonal antibody to single-stranded DNA. *J Pathol*. 2001;193(3):377–382.
25. Maison SF, Emeson RB, Adams JC, Luebke AE, Liberman MC. Loss of alpha CGRP reduces sound-evoked activity in the cochlear nerve. *J Neurophysiol*. 2003;90(5):2941–2949.